

Article ID: 1003 - 6326(2003)02 - 0258 - 04

## Aging transformation in Cu-3.2Ni-0.75Si alloy<sup>①</sup>

ZHAO Dong-mei(赵冬梅)<sup>1, 2</sup>, DONG Qir-ming(董企铭)<sup>2</sup>, LIU Ping(刘平)<sup>2</sup>,KANG Buxi(康布熙)<sup>2</sup>, HUANG Jir-liang(黄金亮)<sup>2</sup>, JIN Zhi-hao(金志浩)<sup>1</sup>

(1. Institute of Materials Science and Engineering, Xi'an Jiaotong University, Xi'an 710049, China

2. Department of Materials Engineering, Luoyang Institute of Technology, Luoyang 471039, China)

**Abstract:** The aging processes in Cu-3.2Ni-0.75Si alloy were examined by means of transmission electron microscope, X-ray diffractometer and high-resolution transmission electron microscopy. It is concluded that before the formation of Ni<sub>2</sub>Si phase there exist continuous phase transformation processes, namely ordering, spinodal decomposition. Thereafter, the solute rich zones form Ni<sub>2</sub>Si phase which is coherent with the matrix.

**Key words:** Cu-Ni-Si alloy; transformation; aging; spinodal decomposition; ordering

**CLC number:** TG 146.1; TG 156.92

**Document code:** A

### 1 INTRODUCTION

Having high strength and good electrical and thermal conductivities, copper alloys are used in a number of engineering applications, such as electric resistance welding electrodes, the liner tube of continuous casting crystallizer, integrated circuit lead frame, aerial conductor of electric locomotive. The representative precipitation-hardenable copper-base alloys for the applications are Cu-Cr<sup>[1]</sup>, Cu-Cr-Zr<sup>[2]</sup>, Cu-Fe-Cr<sup>[3]</sup>, Cu-Ni-Si<sup>[4-6]</sup> etc. Precipitation in Cu-Cr, Cu-Cr-Zr, Cu-Fe-P alloys usually starts from the formation of GP zones, which may be regarded as fully coherent metastable precipitates. Subsequent evolution of the microstructure involves the replacement of the GP zones with more stable phases. This occurs primarily because GP zones are isomorphous with the matrix and therefore, have a lower interfacial energy than intermediate or equilibrium precipitate phases that possess a distinct crystal structure. Furthermore, many experimental results suggest that solute clustering occurs prior to the precipitation of GP zones, and this helps for understanding both the nature and kinetics of the precipitation process<sup>[7-10]</sup>. However, there are still few reports concerning the early stage aging characteristics of Cu-Ni-Si alloy.

The purpose of this paper is to examine the microstructural mechanisms underlying the aging processes and the subsequent various precipitation stages in Cu-Ni-Si alloy. The characteristics of the precipitate have been established by transmission electron microscope (TEM), X-ray diffraction (XD) and high-resolution electron transmission microscopy (HRTEM) have also been used to supplement conventional TEM.

### 2 EXPERIMENTAL

The alloy investigated was prepared by melting copper of 96% purity together with Ni, Si in 10kg medium frequency furnace at the vacuum of about 10<sup>-5</sup> Pa. The composition of the as-cast alloy was Cu-3.2 Ni-0.75Si (%). The ingots were homogenized at 1125 K for 2 h and subsequently rolled at this temperature from a thickness of 22 mm to 2.0 mm. The strip was solution heat treated for 1 h at 1173 K in an argon atmosphere and water quenched. Then it was aged from 723 K to 823K in N<sub>2</sub>+ H<sub>2</sub> atmosphere for various periods up to 2.88 × 10<sup>6</sup> s prior to air cooling. The TEM samples were prepared by conventional electropolishing method using an electrolyte of 20 % HNO<sub>3</sub> (volume fraction) and 80% CH<sub>3</sub>OH (volume fraction) at 233 K. Most of the electron microscopy for this study was carried out using a Philips COM-2000 operated at 200 kV. HREM images of the precipitates were obtained using a JEM 200-CX, microscopy was operated at 200 kV. Tensile tests were carried out on a screw driven AGA-25T testing machine using specimens with a gauge length/height ratio of 5:1 in compliance with the ASTM Standard E8. Strain was measured by a 30 mm automated extensometer and a nominal strain rate of 0.01 min<sup>-1</sup> was employed throughout. An X-ray diffractometer, Y-4Q, was operated in analyzing phase transformation of materials on aging for various times, with scanning speed of 2.4°/min, work voltage and current of 35 kV and 25 mA, radiation of CuK<sub>α</sub> respectively, Ni as filter.

① **Foundation item:** Project(50071026) supported by the National Natural Science Foundation of China

**Received date:** 2002 - 05 - 24; **Accepted date:** 2002 - 08 - 28

**Correspondence:** Associate prof. ZHAO Dong-mei, Tel: + 86 379-5620266; E-mail: lyzdw@371.net

### 3 RESULTS

#### 3.1 Mechanical properties

The effect of aging at 723 K for time between  $0.9 \times 10^3$  s to  $5 \times 10^4$  s on the yield strength and tensile strength is shown in Fig. 1. The increase of the yield stress has no incubation and is followed a plateau in aging curve. Further aging results in further increase of the yield strength and a maximum of the yield strength is reached on aging for  $3.6 \times 10^4$  s. The tensile strength increases rapidly in the first hour and then gradually increases till it reaches a peak on aging for  $1.44 \times 10^4$  s.

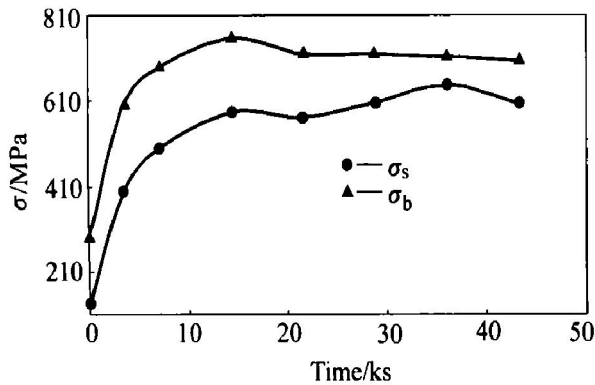


**Fig. 1** Yield strength and tensile strength of Cu-3.2Ni-0.75Si as function of aging time at 723 K

#### 3.2 Microstructure and discussion

Specimens aged at 723 K for 1 000 s were observed to have a modulated structure which produced satellite reflections near (200) diffraction spot and give a striated appearance to images taken with  $g = [200]$  (Fig. 2). Well defined particles were not observed after even the longest aging time of  $7.2 \times 10^3$  s. Attempts were made to measure the average wavelength of the compositional modulations  $\lambda$  from bright-field image taken under two beam condition with  $g = [200]$ . However, the spacings of the intensity variations in the image were found to be random. Examination of the edges of very thin specimens indicated that  $\lambda$  was of the order of 11 nm. This very short wavelength means that even in thin specimens the electron beam is traversing several modulations as it passes through the material, so that the final image intensity is not related in a simple manner to  $\lambda$ . Thus it was not possible to determine  $\lambda$  from the images or even to determine whether it was changing as a function of aging time.

Attempts were also made to measure  $\lambda$  from the position of the (200) satellites spots in electron diffraction patterns, but the satellites were found to be too close to the main spot for accurate measurement as shown in Fig. 2(b).

X - ray diffraction patterns are taken for all

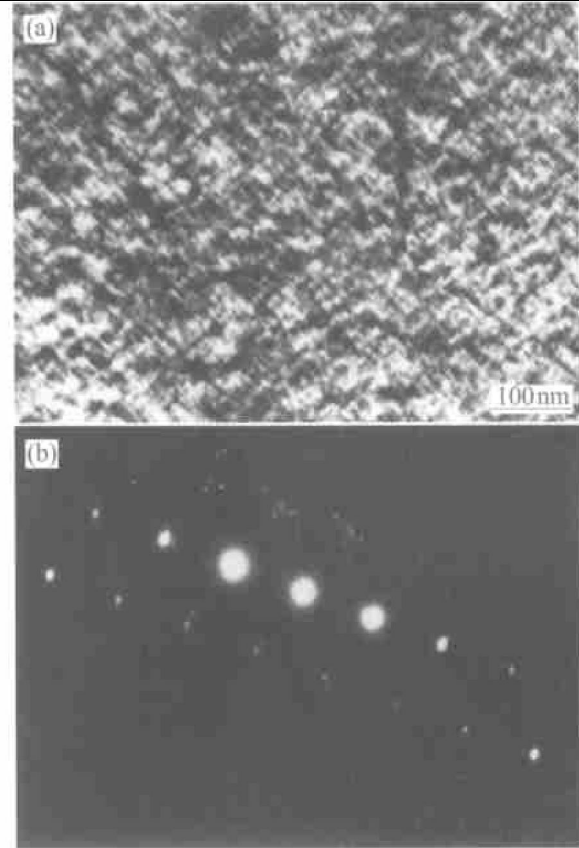


**Fig. 2** Microstructure of Cu-3.2Ni-0.75Si alloy aged at 723 K for 900 s (a), and pattern of aged for 900 s (b)

samples aged for  $0.9 \times 10^3$  s –  $5.76 \times 10^4$  s. Fig. 3 shows the X-ray diffraction patterns of Cu-3.2Ni-0.75Si alloy aged for various durations. After aging for  $1.8 \times 10^3$  s,  $3.6 \times 10^3$  s and  $7.2 \times 10^3$  s, (111) and (200) diffraction peaks broadened, which is a characteristic of spinodal decomposition. The reason of the broadening lies in the formation of poor and rich solute regions in the body during the spinodal decomposition. The lattice value in rich solute regions is less than the average value in poor solute regions. Then around the main diffraction peak, especially the base peak, there will be

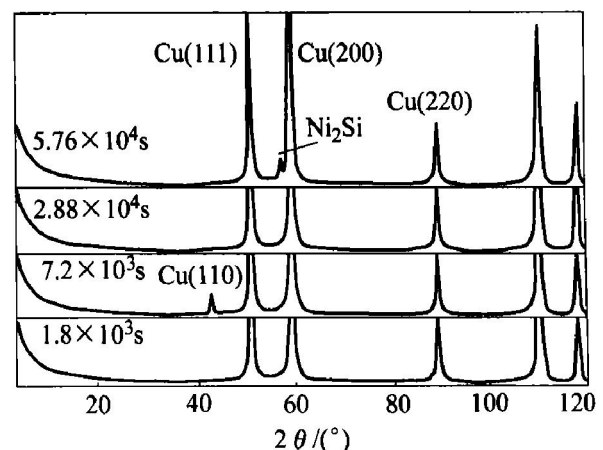


**Fig. 3** XRD patterns of Cu-3.2Ni-0.75Si alloy aged for various durations

found broadened peaks which have similar crystal plane distance with the main diffraction peak. The diffraction angles between the satellite and main diffraction peaks were measured. Then, the Daniel-Lipson equations were used to calculate the spindal wavelength, which are approximately 11.60 nm, 12.75 nm, and 13.00 nm, respectively. Aged for  $7.2 \times 10^3$  s, as spinodal decomposition continues in the supersaturated solid solution, the superlattice diffraction peak appears between  $2\theta = 42^\circ$  to  $45^\circ$ , which suggests that some ordered arrangement should exist in rich-solute region.

After aging for  $7.2 \times 10^3$  s, the amplitude of modulations along  $\langle 100 \rangle$  is in agreement with approximately 25% Si (mole fraction) needed in three dimensional crossing points of  $\langle 100 \rangle$  concentration waves where the ordering particles nucleate later. The structure of the aged sample is shown in Fig. 4 (a). The superlattice spots and sidebands are simultaneously observed in the diffraction patterns. Fig. 4 (b) shows a  $[011]$  diffraction pattern from a specimen aged for  $7.2 \times 10^3$  s. A similar pattern on a Cu-15Ni-8Sn alloy<sup>[11, 12]</sup> confirms the existence of superlattice reflections. An atomic arrangement which has a parent FCC phase and can explain these superlattice reflections is of the  $DO_{22}$ ,  $Al_3Ti$  type<sup>[13, 14]</sup>. The unit cell of the fully ordered crystal would be tetragonal with 8 atoms per cell based on an  $M_3Si$  composition where M is Ni or  $Cu_{1-x}Ni_x$ .

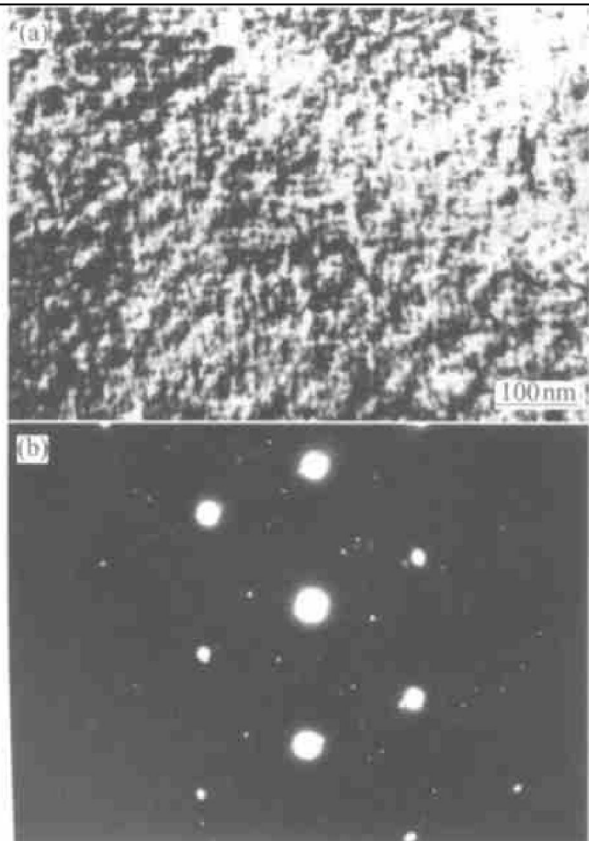


**Fig. 4** Structure of Cu-3.2Ni-0.75Si alloy aged at 723 K for  $7.2 \times 10^3$  s (a) and selected area diffraction of Cu-3.2Ni-0.75Si aged at 723 K for  $7.2 \times 10^3$  s (b)

If the form was approximated as sphere then their radius is about 41 nm. After aging for  $1.44 \times 10^4$  s the sidebands nearly disappear into the matrix spots, the coherent  $\delta-Ni_2Si$  with orthorhombic lattice structure nucleates within the ordering  $(Cu, Ni)_3Si$  (Fig. 5). The diffraction pattern corresponding to this foil orientation is shown in Fig. 5(b). High-resolution electron microscopy was also used to identify the precipitates formed after aging for  $1.44 \times 10^4$  s. The results obtained are shown in Fig. 6. The ordering  $(Cu, Ni)_3Si$ , about 6 nm in size, displays a darker contrast than the surrounding Cu matrix. It can be seen that the  $\delta-Ni_2Si$  appears to be fully coherent with the surrounding ordering  $(Cu, Ni)_3Si$  on  $[011]$   $(Cu, Ni)_3Si$  projection and has the same two-dimensional lattice although lattice distortion exists.

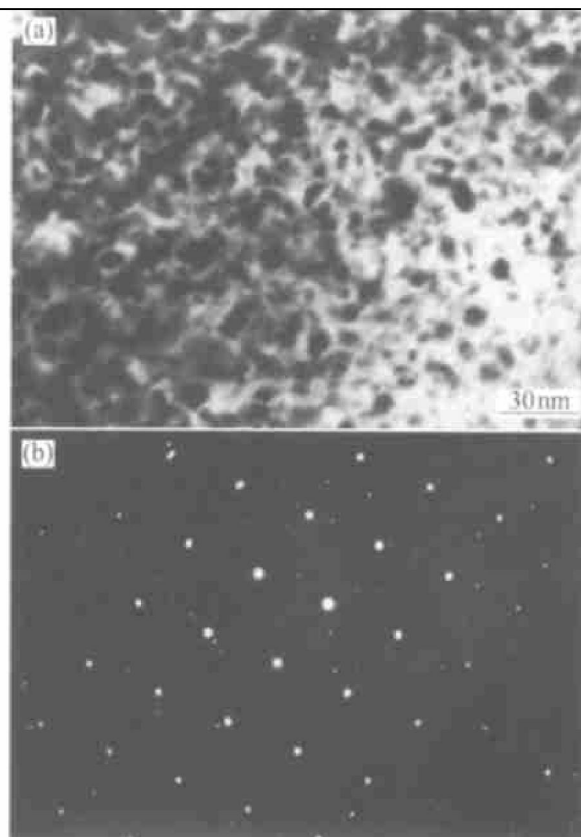


**Fig. 5** Structure of Cu-3.2Ni-0.75Si alloy aged at 723 K for  $1.44 \times 10^4$  s (a) and selected area diffraction of Cu-3.2Ni-0.75Si aged at 723 K for  $1.44 \times 10^4$  s (b)

As previously mentioned, the result for the present study can be summarized that in a Cu-3.2Ni-0.75Si alloy during aging at 723 K, the supersaturated solid solution decomposes by the spinodal mechanism into periodic regions which are Si-rich and Si-poor. The proceeding aging treatment results thus in a ordering metastable phase with the  $DO_{22}[(Cu, Ni)_3Si]$  structure, the  $\delta-Ni_2Si$  phase which has orthorhombic structure appears during further aging.

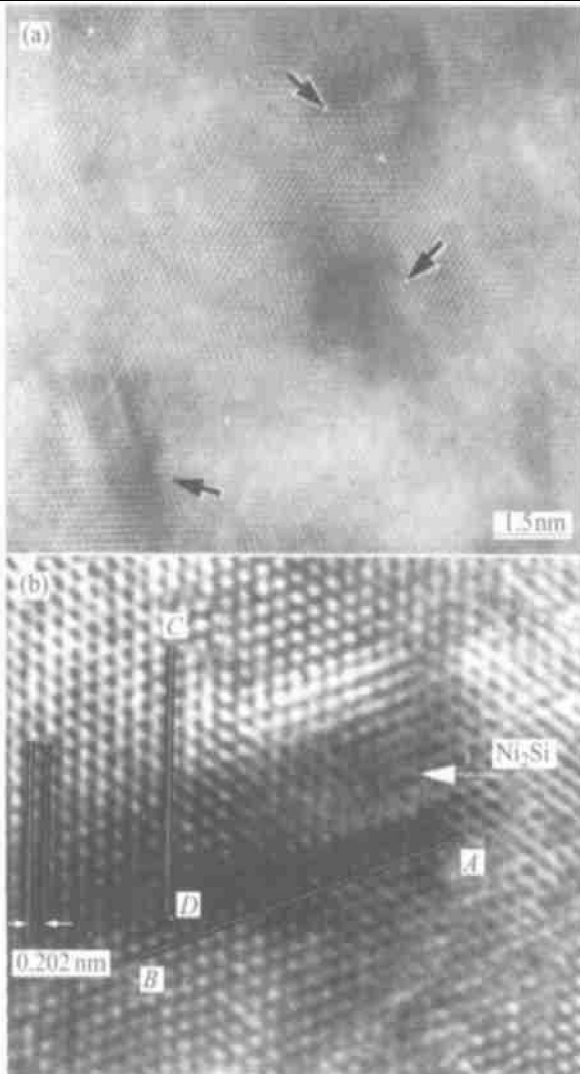


**Fig. 6** High-resolution transmission electron micrographs from peak tensile of Cu-3.2Ni-0.75Si alloy (aged for  $1.44 \times 10^4$  s at 723 K)

(a) —Ordered region;

(b) —Digitized and enlarged view of typical zone showing development of facet labeled AB and CD, approximately parallel to {200} and {111} of  $(\text{Cu, Ni})_3\text{Si}$  ordering phase, respectively.

#### 4 CONCLUSION

When Cu-3.2Ni-0.75Si alloy is aged at 723 K after solution heat treatment, the supersaturated solid solution is appeared following the three stages of decomposition. In the first stage, the modulated structure with Si-rich and Si-poor regions results from spinodal decomposition. In the second

stage, the ordering  $(\text{Cu, Ni})_3\text{Si}$  with  $\text{DO}_{22}$ -type structure nucleates from the modulated structure. In the final stage of transformation a discs structure ( $\text{Cu, Ni}_2\text{Si}$ ) appears.

#### REFERENCES

- [1] Liu P, Kang B X, Cao X G, et al. Strengthening mechanisms in a rapidly solidified and aged Cu-Cr alloy[J]. Journal of Materials Science, 2000, 35: 1691 - 1694.
- [2] Liu P, Kang B X, Cao X G, et al. Aging precipitation and recrystallization of rapidly solidified Cu-Cr-Zr-Mg alloy[J]. Materials Science and Engineering A, 1999, A265: 262 - 267.
- [3] Fernee H, Nairn J, Atrens A. Precipitation hardening of Cu-Fe-Cr alloys[J]. Journal of Materials Science, 2001, 36: 2711 - 2719.
- [4] Lockyer S A, Noble F W. Precipitate structure in a Cu-Ni-Si alloy[J]. Journal of Materials Science, 1994, 29: 218 - 226.
- [5] Lockyer S A. Fatigue of precipitate strengthened Cu-Ni-Si alloy[J]. Materials Science and Technology, 1999, 15 (10): 1147 - 1153.
- [6] Fujiwara H, Kamio A. Effect of alloy composition on precipitation behavior in Cu-Ni-Si alloys[J]. Japan Inst Metals, 1998, 62(4): 301 - 309.
- [7] Jin Y, Adachi K, Takeuchi T, et al. Aging characteristics of Cu-Cr in situ composite[J]. Journal of Materials Science, 1998, 33: 1333 - 1341.
- [8] Ohmori Y S, Nakai I K. Aging behavior of an Al-Li-Cu-Mg-Zr alloy[J]. Metallurgical and Materials Transactions, 1999, 33A(3): 741 - 749.
- [9] Laughlin D E, Cahn J W. Spinodal decomposition in age hardening copper titanium[J]. Acta Metall, 1975, 23 (3): 329.
- [10] Datta A, Soffa W A. The structure and properties of age hardened Cu-Ti alloys[J]. Acta Metall, 1976, 24 (9): 987.
- [11] Zhao J C, Notis M R. Spinodal decomposition, ordering transformation, and discontinuous precipitation in a Cu-15Ni-8Sn alloy[J]. Acta Metall, 1998, 46(12): 4203 - 4218.
- [12] Kratochvil P, Mencl J, Pescka J, et al. The structure and low temperature strength of the age hardened Cu-Ni-Sn alloys[J]. Acta Metall, 1984, 32(9): 1493 - 1497.
- [13] Pearson W B. The Crystal Chemistry and Physics of Metals and Alloys[M]. New York: Wiley-Science, 1972.
- [14] Ditchek B, Schwartz L H. Diffraction study of spinodal decomposition in Cu-10Ni-6Sn[J]. Acta Metall, 1980, 28(6): 807 - 822.

(Edited by HUANG Jin-song)